Purinergic Signalling (2017) 13:559–568
DOI 10.1007/s11302-017-9583-2

ORIGINAL ARTICLE

Nanoparticle-encapsulated emodin decreases diabetic neuropathic pain probably via a mechanism involving P2X3 receptor in the dorsal root ganglia

Lin Li[1,2] · Xuan Sheng[1,2] · Shanhong Zhao[1,2] · Lifang Zou[1,2] · Xinyao Han[3] · Yingxin Gong[3] · Huilong Yuan[1,2] · Liran Shi[1,2] · Lili Guo[1,2] · Tianyu Jia[1,2] · Shuangmei Liu[1,2] · Bing Wu[1,2] · Zhihua Yi[1,2] · Hui Liu[1,2] · Yun Gao[1,2] · Guilin Li[1,2] · Guodong Li[1,4] · Chunping Zhang[2,5] · Hong Xu[1,2] · Shangdong Liang[1,2]

Received: 20 May 2017 / Accepted: 10 August 2017 / Published online: 24 August 2017

Abstract Diabetic peripheral neuropathy (DPN) is the most common complication of diabetes mellitus (DM). More than 90% of all cases of DM belong to type 2 diabetes mellitus (T2DM). Emodin is the main active component of *Radix et rhizoma rhei* and has anti-bacterial, anti-viral, anti-ulcerogenic, anti-inflammatory, and anti-cancer effects. Nanoparticle encapsulation of drugs is beneficial for drug targeting and bioavailability as well as for lowering drug toxicity side effects. The aim of this study was to investigate the effects of nanoparticle-encapsulated emodin (nano emodin) on diabetic neuropathic pain (DNP) mediated by the Purin 2X3 (P2X3) receptor in the dorsal root ganglia (DRG). Mechanical withdrawal threshold (MWT) and thermal withdrawal latency (TWL) values in T2DM rats were lower than those of control rats. MWT and TWL in T2DM rats treated with nano emodin were higher compared with those in T2DM rats. Expression levels of P2X3 protein and messenger RNA (mRNA) in the DRG of T2DM rats were higher than those of controls, while levels in T2DM rats treated with nano emodin were significantly lower than those of the T2DM rats. Phosphorylation and activation of ERK1/2 in the T2DM DRG were decreased by nano emodin treatment. Nano emodin significantly inhibited currents activated by the P2X3 agonist α,β-meATP in HEK293 cells transfected with the P2X3 receptor. Therefore, nano emodin treatment may relieve DNP by decreasing excitatory transmission mediated by the DRG P2X3 receptor in T2DM rats.

Keywords P2X3 receptor · Diabetic peripheral neuropathy · Dorsal root ganglia · Nanoparticle-encapsulated emodin

Abbreviations

DPN	Diabetic peripheral neuropathy
T2DM	Type 2 diabetes mellitus
α,β-meATP	α,β-Methyleneadenosine 5′-triphosphate
DRG	Dorsal root ganglia
MWT	Mechanical withdrawal threshold
TWL	Thermal withdrawal latency
Nano emodin	Nanoparticle-encapsulated emodin
IOD	Integrated optical density

Introduction

Diabetes mellitus (DM) is a major cause of peripheral neuropathy. The global prevalence of DM in 2011 was approximately 366 million (8.3%), and prevalence is expected to increase to 552 million (9.9%) by 2030 [1]. More than 90% of all cases of DM belong to type 2 diabetes mellitus (T2DM). Diabetic neuropathic pain (DNP) is the most common complication of T2DM. DNP leads to dysfunction in the dorsal root ganglia (DRG) [2–4]. Toxicity of hyperglycaemia is associated with

✉ Shangdong Liang
liangsd@hotmail.com

1 Department of Physiology, Medical School of Nanchang University, Nanchang 330006, Jiangxi, People's Republic of China

2 Jiangxi Provincial Key Laboratory of autonomic nervous function and disease, Nanchang 330006, Jiangxi, People's Republic of China

3 First Clinical Department, Medical School of Nanchang University, Nanchang 330006, Jiangxi, People's Republic of China

4 Department of Clinical Translational Research, Singapore General Hospital, Singapore, Singapore

5 Department of Cell Biology, Medical School of Nanchang University, Nanchang 330006, Jiangxi, People's Republic of China

local metabolic changes in T2DM [3, 5]. Long-standing hyperglycemia destroys the homeostasis of peripheral tissues and causes peripheral nerve injury [6]. DNP includes spontaneous pain, allodynia (pain to normally innocuous stimuli), and hyperalgesia (increased pain perception to noxious stimuli) [3, 4, 7, 8]. As a chronic peripheral neuropathy, DNP has a substantial impact on the quality of life of diabetic patients. The pathogenesis of DPN remains uncertain, and its mechanism is complex and multi-factorial. At present, no specific medication is available for DNP treatment [7, 9, 10].

Adenosine-5′-triphosphate (ATP) is an endogenous ligand that can act on ionotropic P2X receptors, which are involved in the transmission of painful sensory information from the periphery to the central nervous system (CNS). The P2X3 receptor is most highly expressed in a subpopulation of small diameter primary afferent neurons. The expression of P2X3 protein and messenger RNA (mRNA) is increased following chronic constriction injury (CCI) of the sciatic nerve [11–18]. The P2X3 receptor plays a crucial role in chronic neuropathic pain [11–13, 15–19], and this receptor has been shown to mediate mechanical allodynia in diabetic neuropathic rats [20]. Therefore, the P2X3 receptor is a suitable target for analgesic drugs in DNP. Emodin (3-methyl-1,6,8-trihydroxyanthraquinone) is a naturally occurring anthraquinone derivative isolated from *Radix et rhizoma rhei* that has anti-nociceptive, anti-inflammatory, and anti-cancer effects. Nanoparticle encapsulation of drugs is beneficial for drug targeting and bioavailability and for lowering drug toxicity side effects. In this study, we investigated the effects of nanoparticle-encapsulated emodin (nano emodin) on DNP involved in the P2X3 receptor in rat DRG neurons of T2DM model.

Materials and methods

Animals and animal groups

Male Sprague-Dawley (SD) rats (180–230 g) were provided by the Center of Laboratory Animal Science of Nanchang University. The animals were housed in plastic boxes in groups of three at 21–25 °C. The International Association for the Study of Pain (IASP)'s ethical guidelines for pain research in animals were followed. Type 2 diabetic rat models were induced by a single intraperitoneal (i.p.) injection of 30 mg/kg streptozocin (STZ) and a diet of high calorie food [21, 22]. STZ was dissolved in citrate buffer (pH 4.5). The control animals received pure buffer. After 7 days, blood samples were obtained from the tail vein, and glycaemia was determined using a glucometer. Fasting blood glucose > 200 mg/dl (11.1 mM) was considered a marker of DM [21, 22]. Spontaneous pain behaviors were measured at 7 days after STZ injection. At day 14, the animals were sacrificed by CO_2 inhalation, and the L4–5 DRG was removed.

The rats were assigned in a random blinded manner to one of the four following groups: the control group (control group), the diabetic model group (DM group), the nanoparticle-encapsulated emodin-treated diabetic rat group (DM + nano emodin group), and the nanoparticle encapsulation carrier-treated diabetic rat group (DM + nanocarrier group). Each group contained 8–10 animals. Nano emodin (5 mg/ml per rat, containing 1 mg pure emodin) or nanocarrier was injected into the sublingual vein (every other day for a total of three injections) before the experiment.

Synthesis of poly-PEGMA-DMAEMA-MAMMAM nano macromolecule

Biological nanocarriers can not only improve the solubility and bioavailability of a drug but can also control drug release and attenuate toxic side effects. Reversible addition fragmentation chain transfer (RAFT) radical polymerization has developed into an extremely versatile controlled/living free radical polymerization technique, allowing a wide range of reaction conditions and applicable monomers. A typical protocol for the synthesis of an amphiphilic polymer macromolecule (PEGMA-DMAEMA-MAMMAM) was conducted through RAFT solution polymerization. PEGMA served as the hydrophilic segment, MAMMAM served as a hydrophobic block, and DMAEMA served as a segment to bind DNA. Briefly, CTA (0.5 mmol), AIBN (0.05 mmol), DMAEMA (5 mmol), PEGMA (10 mmol), and MAM (10 mmol) were added to a 50-ml round-bottomed flask. Methylbenzene (20 ml) was added to homogenize the solution, which was then purged with nitrogen for 30 min. The sealed flask was immersed in an oil bath at 55 °C for 24 h under nitrogen conditions. The polymerization was subsequently dried under vacuum rotary steam. The block copolymer was purified by dialysis against distilled water/ethanol for 48 h (MWCO 3500) and recovered by freeze-drying. Purified PEGMA-DMAEMA-MAM was obtained as a yellow solid.

Synthesis of emodin-loaded poly-PEGMA-DMAEMA-MAM microspheres

To combine the advantages of biological nanocarriers and the benefits of emodin, emodin-polybutylcyanoacrylate nanoparticles were prepared using anionic emulsion polymerization. A typical oil-in-water (O/W) solvent evaporation method was used to prepare the microspheres. Emodin (50 mg) was dissolved in 16 ml of absolute ethyl alcohol. Poly-PEGMA-DMAEMA-MAM (60 mg) was dissolved in 6 ml of acetone. Then, the two solutions were mixed to obtain two-phase organic solvents. The organic solvents were immersed in distilled water (100 ml, pH 5.0) at 2 ml/min under an ice bath.

The organic phase was emulsified with a homogenizer into the aqueous phase. The dispersion was then evaporated at ambient temperature and pressure to harden the microspheres. The microspheres were separated by filtration, vacuum dried, weighed, and stored in a vacuum desiccator.

Measurement of the MWT

The mechanical nociceptive threshold was evaluated by observing withdrawal responses to mechanical stimulation using von Frey filaments (Stoelting, Wood Dale, IL, USA) [22–24]. The von Frey filament was used to apply a linearly increasing pressure, starting at 0.13 g and increasing until a withdrawal response occurred. The pressure was applied through a cone-shaped plastic tip with a diameter of 1 mm onto the dorsal surface of the hind paws. The tip was positioned between the third and fourth metatarsus, and force was applied until the rat attempted to withdraw its paw (paw withdrawal threshold to pressure). The hind paws were alternated at 2-min intervals. The pain threshold was calculated as the mean of three consecutive stable values, as expressed in grams, and was determined by a blinded observer.

Measurement of the TWL

The latency to hind paw withdrawal from a thermal stimulus was determined by exposing the plantar surface of the hind paw to radiant heat using the Thermal Paw Stimulation System (BME-410C, Tianjin, China) [22–24]. Rats were placed in a transparent, square, bottomless acrylic box (22 cm × 12 cm × 22 cm) on a glass plate under which a light was located. After a 30-min habituation period, the plantar surface of the paw was exposed to a beam of radiant heat applied through the glass floor. Activation of the bulb simultaneously activated a timer, and both were immediately turned off by paw withdrawal or at the 25-s cutoff time. A blinded observer tested the hind paw withdrawal in triplicate at 5-min intervals.

Real-time RT-PCR

Rats in the four groups were anesthetized with 10% chloral hydrate (3 ml/kg, i.p.). The L4–6 DRGs were isolated immediately and flushed with ice-cold PBS. Total RNA samples were prepared from the L4–6 DRGs of each group using TRIzol Total RNA Reagent (Beijing Tiangen Biotech Co., China). Complementary DNA (cDNA) synthesis was performed with 2 μg of total RNA using the RevertAid™ H Minus First Strand cDNA Synthesis Kit (Fermentas, Burlington, Ontario, Canada). The primers were designed with Primer Express 3.0 software (Applied Biosystems), and the sequences were as follows: P2X3, forward 5′-GAGT CCGAGGCAATCTAATG-3′; reverse 5′-CTGT GATCCCAACAAAGGTC-3′; β-actin, forward 5′-TAAA GACCTCTATGCCAACACAGT-3′, reverse 5′-GGGG TGTTGAAGGTCTCAAA-3′. Quantitative PCR was performed using SYBR® Green MasterMix in an ABI PRISM® 7500 Sequence Detection System (Applied Biosystems Inc., Foster City, CA). Quantification of gene expression was performed using the ΔΔCT calculation with CT as the threshold cycle. The relative levels of the target genes, normalized to the sample with the lowest CT, were reported as $2^{-\Delta\Delta CT}$ [25].

Western blotting

Animals were anesthetized with sodium pentobarbital, the DRG were dissected, and approximately 6–10 samples were harvested from each rat. The DRG were isolated immediately and rinsed in ice-cold phosphate-buffered saline (PBS) [24]. After dilution with sample buffer (250 mmol/L Tris-Cl, 200 mmol/L dithiothreitol, 10% sodium dodecyl sulfate (SDS), 0.5% bromophenol blue, and 50% glycerol) and heating to 95 °C for 10 min, 20-μg samples of total protein were separated for P2X3 receptor analysis using 10% SDS-polyacrylamide gel electrophoresis and transferred onto a polyvinylidene difluoride membrane. After incubation with a primary antibody against the P2X3 receptor (1:1000 ratio, Abcam, USA), rabbit polyclonal anti-tumor necrosis factor alpha (TNF-α)-receptor 1 (anti-TNF-α-R1, 1:800 ratio, Abcam, USA), the membrane was incubated with peroxidase-conjugated secondary antibodies (Cell Signaling Technology, Danvers, MA, USA). Immunodetection was performed using the Pierce enhanced chemiluminescence substrate (Thermo Scientific, Waltham, MA, USA). β-Actin antibody (1:10,000 ratio, Santa Cruz Biotechnology, Santa Cruz, CA, USA) was used as a loading control. Band densities were normalized to each β-actin internal control.

The expression levels of the extracellular regulated kinase 1/2 (ERK1/2) and phosphorylated-ERK1/2 (p-ERK1/2) proteins were tested using the same protocol employed for the P2X3 protein. The primary antibodies and dilutions used were the following: rabbit polyclonal anti-phospho-p44/42 MAPK (ERK1/2, 1:1000 ratio, Cell Signaling Technology, USA) and rabbit polyclonal anti-p44/42 MAPK (ERK1/2, 1:1000 ratio, Cell Signaling Technology, USA).

HEK293 cell transfection

Human embryonic kidney (HEK) 293 cells were grown in Dulbecco's modified Eagle's medium supplemented with 10% fetal bovine serum and 1% penicillin/streptomycin at 37 °C in a humidified atmosphere containing 5% CO_2. Cells were transiently transfected with the human pcDNA3.0-EGFP-P2X3 plasmid using Lipofectamine 2000 reagent

(Invitrogen) according to the manufacturer's instructions. When HEK293 cells were 70–80% confluent, cell culture media was replaced with OptiMEM; transfection was performed 2 h later. The transfection medium was prepared as follows: (a) 4 μg plasmid DNA was diluted with OptiMEM to 250 μl final volume; (b) 10 μl Lipofectamine 2000 was diluted with OptiMEM to 250 μl final volume; and (c) the Lipofectamine-containing solution was mixed with the plasmid-containing solutions and incubated at room temperature for 20 min. Subsequently, 500 μl of cDNA/lipofectamine solution was added to each well. The cells were incubated for 6 h at 37 °C and 5% CO_2. After incubation, the cells were washed in MEM containing 10% FBS and incubated for 24–48 h. GFP fluorescence was assessed as a reporter for the efficiency of transfection [26]. Whole-cell patch clamp recordings were carried out 1–2 days after transfection.

Electrophysiological recordings

Electrophysiological recording was carried out by using a patch/whole cell clamp amplifier (Axopatch 200B) [26]. HEK293 cells expressing green fluorescence were subjected to electrophysiological recording. Microelectrodes were filled with internal solution composed of 145 mM K gluconate, 0.75 mM EGTA, 10 mM HEPES, 0.1 mM $CaCl_2$, 2 mM MgATP, and 0.3 mM Na_3GTP. The bath was continuously perfused with extracellular solution containing 126 mM NaCl, 2.5 mM KCl, 10 mM glucose, 1.2 mM $MgCl_2$, 2.4 mM $CaCl_2$, and 18 mM $NaHCO_3$. The osmolarity of the extracellular solution and internal solution was adjusted to 340 mOsm with sucrose. The pH of the extracellular solution was adjusted to 7.4 with NaOH while the internal solution was adjusted to 7.3 with KOH. The resistance of recording electrodes was 2–6 MΩ. A small patch of membrane underneath the tip of the pipette was aspirated to form a seal (1–10 GΩ), and then a more negative pressure was applied to rupture it. The holding potential (HP) was set at −70 mV. α,β-Methylene ATP (α,β-meATP, Sigma) or A-317491 (Sigma) was dissolved in the extracellular solution. Nano emodin (0.5 μg/ml, 1.85 μM) and other drugs were applied rapidly through a manifold composed of 10 capillaries made of fused silica coated with polyimide, with 200 μm internal diameter. The distance from the tubule mouth to the examined cell was approximately 100 μm. One barrel was used to apply drug-free extracellular solution to enable rapid termination of drug application. The drugs were dissolved in external solution and delivered by gravity flow from an array of tubules (500 μm o.d., 200 μm i.d.) connected to a series of independent reservoirs. Rapid solution-exchange was achieved by shifting the tubules horizontally with a micromanipulator. The time of solution exchange was approximately 20–30 ms as confirmed by liquid junction potential measurements. Drugs were separately applied for 2 s at 4 min intervals, a protocol that was sufficient for responses to be reproducible. Data were low-pass filtered at 2 Hz, digitized at 5 kHz, and stored at a laboratory computer using Digidata 1200 interface and pClamp10.0 software (Axon Instruments).

Statistical analysis

The data were statistically analyzed using SPSS 11.5. All results are expressed as the mean ± SEM. Statistical significance was determined by one-way analysis of variance (ANOVA) followed by Fisher's post hoc tests for multiple comparisons. A value of $p < 0.05$ was considered significant.

Results

Effects of nano emodin on mechanical and thermal hyperalgesia in DM rats

The mechanical withdrawal threshold (MWT) was measured. The MWT in the DM group was lower than in the control group ($p < 0.01$). The MWT in DM rats treated with nano emodin (5 mg/ml per rat, containing 1 mg pure emodin) was higher than in the DM rats ($p < 0.01$) (Fig. 1a). There was no difference between the DM group and DM + nanocarrier group ($p > 0.05$). The above results showed that nano emodin inhibited pain behaviors by increasing the mechanical hyperalgesia threshold in DM rats.

The thermal withdrawal latency (TWL) was also measured. The TWL in the DM group was lower than in the control group ($p < 0.01$). The TWL in DM rats treated with nano emodin was higher than the DM rats ($p < 0.01$) (Fig. 1b). There was no difference between the DM group and DM + nanocarrier group ($p > 0.05$). The above results indicated that nano emodin treatment also elevated the thermal hyperalgesia threshold in DM rats, suggesting that nano emodin treatment relieved neuropathic pain.

Effects of nano emodin on expression levels of P2X3 mRNA and protein in the DRG of DM rats

The expression levels of P2X3 mRNA in the DRG of each group were studied by real-time RT-PCR. These assays showed that relative levels of P2X3 mRNA in the DM group were significantly increased compared to the control group ($p < 0.01$, $n = 8$ for each group). The levels of P2X3 mRNA in DM rats treated with nano emodin were significantly decreased compared to the DM group ($p < 0.05$, $n = 8$ for each group). There were no differences in the expression of P2X3 mRNA when comparing the DRG from the DM group and DM + nanocarrier group ($p > 0.05$, $n = 8$ for each group) (Fig. 2a). These results indicate that nano emodin treatment

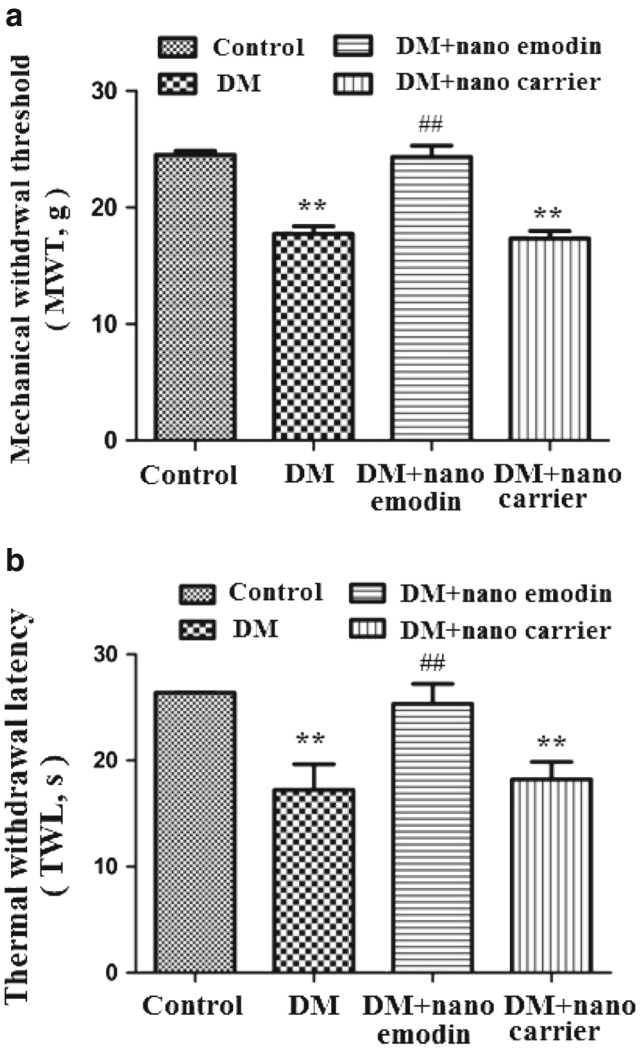

Fig. 1 Effect of nano emodin on mechanical withdrawal threshold and thermal withdrawal latency in T2DM rats. **a**. The mechanical withdrawal threshold (MWT) in T2DM rats treated with nano emodin (5 mg/ml per rat, containing 1 mg pure emodin) was higher than in T2DM rats ($p < 0.01$). There was no difference between the DM group and DM + nanocarrier group ($p > 0.05$). The upper limit of MWT detection was 26.0 g. Results are expressed as mean ± SEM, $n = 8$, $^{*}p < 0.05$, $^{**}p < 0.01$ compared to the control group; $^{\#}p < 0.05$, $^{\#\#}p < 0.01$ compared to the DM group. **b**. The thermal withdrawal latency (TWL) in DM rats treated with nano emodin was higher than in DM rats ($p < 0.01$). There was no difference between the DM group and DM + nanocarrier group ($p > 0.05$). The upper limit of TWL detection was 30 s. Results are expressed as mean ± SEM, $n = 8$, $^{*}p < 0.05$, $^{**}p < 0.01$ compared to the control group; $^{\#}p < 0.05$, $^{\#\#}p < 0.01$ compared to the DM group

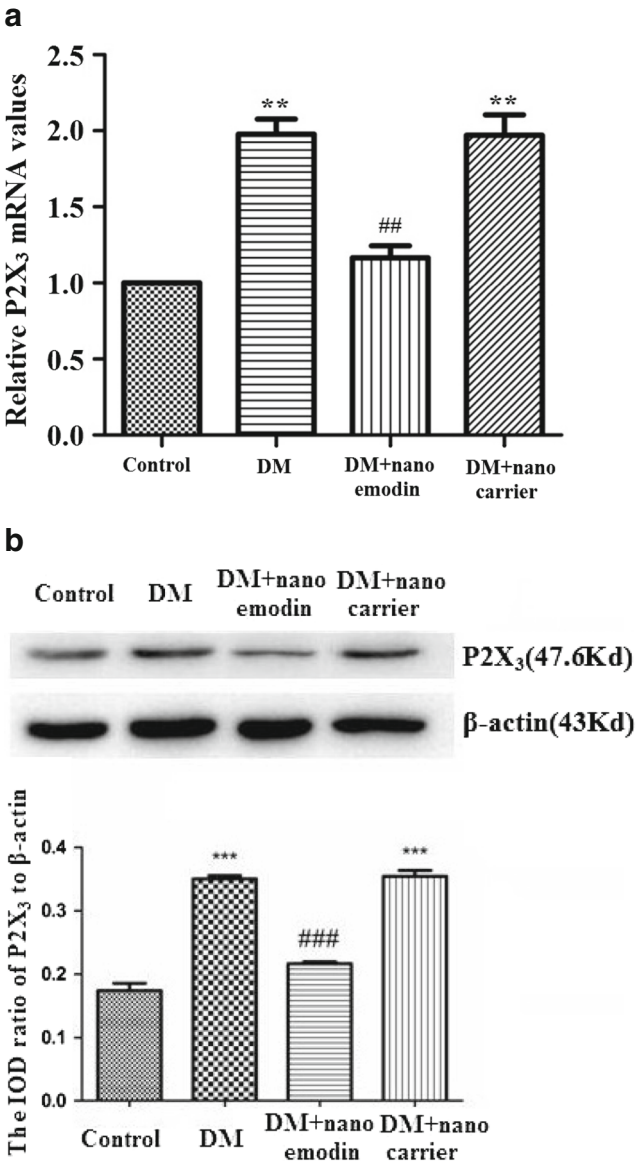

Fig. 2 Effect of nano emodin on the expression of P2X3 mRNA and protein in the DRG of T2DM rats. **a.** Expression of P2X3 mRNA was examined using real time RT-PCR. Expression levels of P2X3 mRNA in the T2DM group were higher than in the control group ($p < 0.05$, $n = 8$ for each group). Levels of P2X3 mRNA in T2DM rats treated with nano emodin were significantly lower than in the untreated T2DM group ($p < 0.05$, $n = 8$ for each group). There were no differences in expression levels of P2X3 mRNA when comparing the DRG from the DM group and DM + nanocarrier group ($p > 0.05$, $n = 8$ for each group). Results are expressed as mean ± SEM, $n = 10$. $^{**}p < 0.01$ compared to the control group; $^{\#\#}p < 0.01$ compared to the DM group. **b.** The expression of P2X3 protein in the DRG was examined using Western blots. Image analysis revealed that levels (assessed by integrated optical density) of P2X3 protein (normalized to each β-actin internal control) in the DM group were higher than in the control group. Levels of P2X3 protein in T2DM rats treated with nano emodin were significantly lower than in the DM group. There were no differences in the levels of P2X3 protein when comparing DRG from the DM group and DM + nanocarrier group. Results are expressed as mean ± SEM, $n = 10$. $^{**}p < 0.01$ compared to the control group; $^{\#\#}p < 0.01$ compared to the DM group

may reduce the upregulated expression of P2X3 mRNA in the DRG of DM rats.

The expression of P2X3 protein in the DRG was further studied by Western blotting. Image analysis demonstrated that the levels (average optical density) of P2X3 protein (normalized to each β-actin internal control) in the DM group were higher than those in the control group ($p < 0.05$, $n = 8$ for each group). The levels of P2X3 protein in DM rats treated with

nano emodin were significantly lower than those in the DM group ($p < 0.05$, $n = 8$ for each group). There were no differences in the expression of P2X3 protein when comparing the DRG from the DM group and DM + nanocarrier group ($p > 0.05$, $n = 8$ for each group) (Fig. 2b). These results indicate that nano emodin treatment may decrease the expression of DRG P2X3 protein in DM rats.

Effects of nano emodin on expression of TNF-R1 protein in the DRG of DM rats

TNF-R1 in DRG neurons is activated by tumor necrosis factor alpha (TNF-α). The levels of TNF-R1 protein in the DRG were analyzed by Western blotting. According to image analyses, the levels of TNF-R1 protein (normalized to each β-actin internal control) in the DM group were significantly augmented compared to the control group ($p < 0.01$). The relative levels of TNF-R1 protein in the DM + nano emodin group were lower than those in the DM group ($p < 0.01$) (Fig. 3). There were no differences in the expression of TNF-R1 protein when comparing the DRG from the DM group and DM + nanocarrier group ($p > 0.05$, $n = 8$ for each group) (Fig. 3).

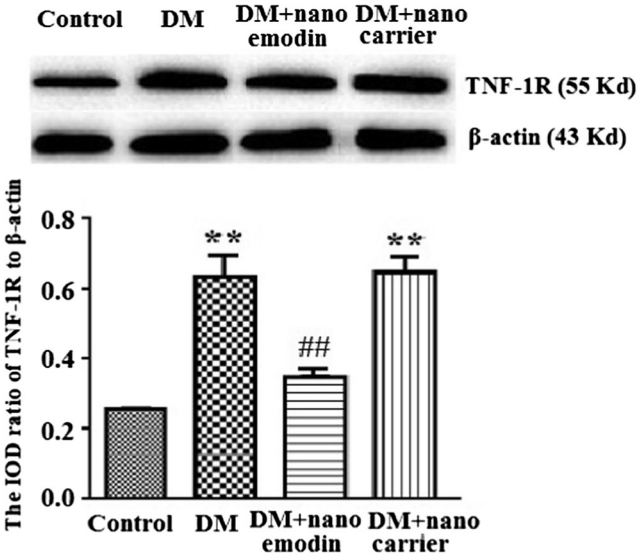

Fig. 3 Effects of nano emodin on the expression of TNF-R1 protein in the DRG of T2DM rats. Image analysis indicated that levels (assessed by integrated optical density) of TNF-R1 protein (normalized to each β-actin internal control) in the DM group were higher than in the control group. Expression levels of TNF-R1 protein in DM rats treated with nano emodin were significantly lower than in the DM group. There were no differences in TNF-R1 protein expression between DRG from the DM group and DM + nanocarrier group. Results are expressed as mean ± SEM, $n = 10$. $^{**}p < 0.01$ compared to the control group; $^{\#\#}p < 0.01$ compared to the DM group

Effects of nano emodin on levels of ERK1/2 and p-ERK1/2 in the DRG of DM rats

The phosphorylation and activation of ERK1/2 participates in neuropathic pain. Levels of ERK1/2 and p-ERK1/2 in the DRG were analyzed by Western blotting. The integrated optical density (IOD) ratio of ERK1/2 to β-actin did not significantly differ between the DM group and the control group ($p > 0.05$). However, the IOD ratio of p-ERK1/2 to ERK1/2 ($n = 8$) in the DM group was higher than in the control group ($p < 0.05$, $n = 8$ for each group) (Fig. 4). These results indicated that the role of ERK phosphorylation in the DRG was related to P2X3 receptor-mediated hyperalgesia in DM rats.

In addition, we examined whether the administration of nano emodin could affect the phosphorylation of ERK in the DM DRG. The IOD ratio of p-ERK1/2 to ERK1/2 in the DM rats treated with nano emodin was significantly lower than in the DM group ($p < 0.05$, $n = 8$ for each group). There were no differences in the IOD ratio of p-ERK1/2 to β-actin between the DM group and the DM + nanocarrier group ($p > 0.05$, $n = 8$ for each group) (Fig. 4). Activation of the ERK pathway participates in P2X3 receptor-mediated neuropathic pain [27, 28]. Thus, these results suggest that nano emodin treatment may decrease phosphorylation of ERK1/2 in the DRG of DM rats to alleviate P2X3 receptor-mediated hyperalgesia.

Effects of nano emodin on α,β-meATP-activated currents in HEK293 cells transfected with the hP2X3 receptor

To determine the direct effect of nano emodin on the P2X3 receptor, pcDNA3.0-EGFP-P2X3 plasmids were transiently transfected into HEK293 cells. Currents activated by the P2X3 agonist α,β-meATP (5 μM) in HEK293 cells transfected with the pEGFP-hP2X3 plasmid were recorded by whole-cell patch clamp. As represented in Fig. 5, HEK293 cells expressing the P2X3 receptor can be activated by α,β-meATP. Nanocarrier has no inhibition effect to α,β-meATP-activated current, and normal emodin (30 μM) decreased α,β-meATP-activated current by 50% (Fig. 5a). Nano emodin (1.85 μM) significantly inhibited α,β-meATP (5 μM)-activated current in HEK293 cells expressing the P2X3 receptor ($p < 0.01$) (Fig. 5b), and the inhibition effect is concentration dependent with the IC_{50} 1.87 ± 0.47 (Fig. 5c). These results indicated that nano emodin inhibited α,β-meATP-activated currents in HEK293 cells expressing the P2X3 receptor. The inhibition effect of nano emodin is stronger compared with normal emodin (30 μM).

Discussion

T2DM is a complex and heterogeneous disorder presently affecting more than 90% of all cases of DM. Neuropathy symptoms in DM are likely related to TRPA1 receptors [29],

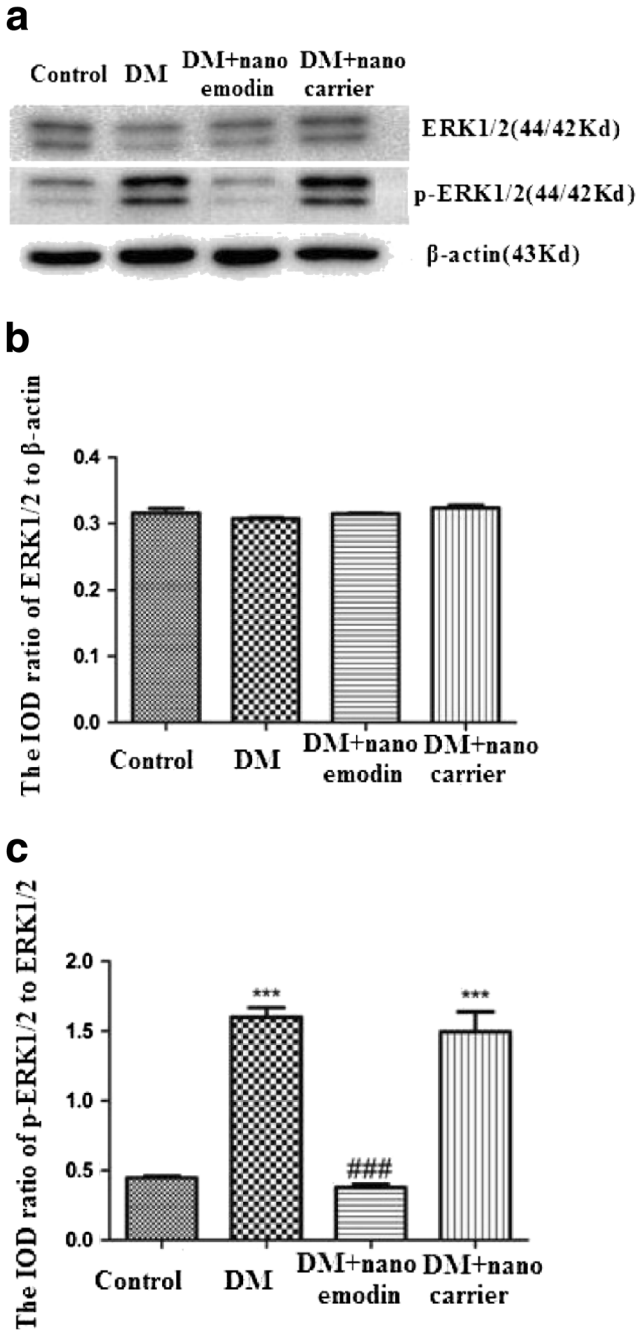

Fig. 4 Effects of nano emodin on levels of ERK1/2 and p-ERK1/2 in the DRG of T2DM rats. **a.** Expression levels of ERK1/2 and p-ERK1/2 in the DRG were analyzed using Western blots. **b**. The integrated optical density (IOD) ratio of ERK1/2 to β-actin was not significantly different between the two groups ($p > 0.05$). **c**. The IOD ratio of p-ERK1/2 to ERK1/2 in the DM group was higher than in the control group ($n = 8$). The IOD ratio of p-ERK1/2 to ERK1/2 in DM rats treated with nano emodin was significantly lower than in the DM group ($p < 0.05$, $n = 8$ for each group). There was no difference in the IOD ratio of p-ERK1/2 to ERK1/2 between the DM group and DM + nanocarrier group ($p > 0.05$, $n = 8$ for each group). Results are expressed as mean ± SEM, $n = 8$. $^{*}p < 0.05$ compared to the control group; $^{\#}p < 0.05$ compared to the DM group

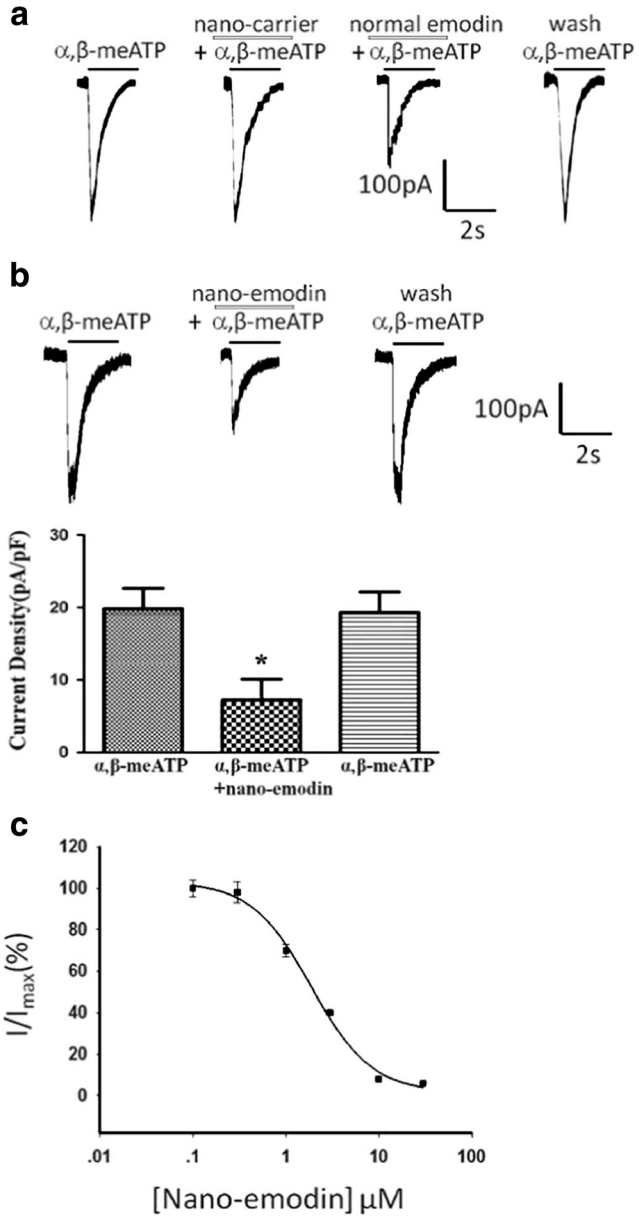

Fig. 5 Effects of nano emodin on α,β-meATP-activated current in HEK293 cells transfected with the hP2X3 receptor. **a.** α,β-meATP (5 μM) activated the currents in HEK293 cells transfected with the hP2X3 receptor. Nanocarrier has no inhibition effect to α,β-meATP-activated current. Normal emodin (30 μM) decreased α,β-meATP-activated current by 50%. **b.** Original tracings indicate that nano emodin (1.85 μM) primarily decreased α,β-meATP (5 μM)-induced currents by 60%. The histogram shows current density with different drugs. Data are presented as the means ± SEM of eight cells per group. $^{*}p < 0.05$ compared with α,β-meATP alone. **c.** The photo shows the concentration-response curves for nano emodin against α,β-meATP (5 μM) with the IC_{50} 1.87 ± 0.47

and STZ-induced mechanical allodynia is mediated by P2X3 receptors in the DRG neurons [20]. DNP is a common complication of T2DM [3, 26, 30–32]. Our results showed that thermal hyperalgesia and abnormal mechanical hyperalgesia in DM rats were increased compared with those in control rats.

T2DM is often accompanied by a low-grade inflammation. As an inflammatory mediator, ATP activates P2X3 receptors and induces neuropathic pain [11–14, 33, 34]. The P2X3 receptor is expressed in small diameter neurons of the DRG [11, 14–17, 19, 34]. Damage to peripheral nerves in neuropathic pain state can enhance expression levels of the P2X3 receptor [11, 14–16, 34]. The present study demonstrated that the expression of P2X3 protein and mRNA in the T2DM DRG is upregulated compared to controls. Thus, enhanced thermal hyperalgesia and mechanical hyperalgesia were associated with upregulated expression of P2X3 mRNA and protein in the DRG of the T2DM group. In addition, pharmacologic treatment of chronic DNP is a challenge for researchers.

Emodin has limited clinical application due to its poor water solubility, which makes it difficult to absorb. Nanoscale drug carriers ameliorate the pharmacokinetics and bioavailability of therapeutic agents, decrease toxicity, facilitate intracellular delivery, and prolong their effective time. The bioavailability of emodin was improved after formulation into biodegradable nanoparticles. The present study demonstrated that expression levels of DRG P2X3 protein and mRNA in DM rats treated with nano emodin were significantly lower than in untreated DM rats. Additionally, MWT and TWL in DM rats treated with nano emodin were significantly higher than in untreated DM model rats. These findings suggested that nano emodin treatment decreased mechanical and thermal hyperalgesia in T2DM rats. Therefore, nano emodin treatment may relieve P2X3 receptor-mediated DNP in DRG primary sensory neurons. The concentration of the nano emodin in this study was only 1 mg/ml per rat, which was significantly lower than the common dose of 20–80 mg/kg [35].

TNF-α is a pro-inflammatory cytokine that has an important role in the initiation and maintenance of neuropathic pain [36]. TNF-α can activate TNF-R1 in DRG neurons and enhance neuronal excitability. In this study, expression levels of TNF-R1 in the DRG of T2DM rats were higher than in the control group. TNF-α and TNF-R1 have a pivotal role at both peripheral and central levels of sensitization, and TNF-α potentiates P2X3 receptor-mediated pain sensations [37]. ATP stimulates TNF-α release and further TNF-α facilitates ATP release; the abundant ATP activates P2X3 receptors and amplifies nociceptive signaling [27, 28]. Thus, TNF-α may activate TNF-R1 in DRG neurons to exacerbate mechanical and thermal hyperalgesia in T2DM rats. In T2DM rats treated with nano emodin, upregulation of TNF-R1 in the DRG was significantly lower than in untreated T2DM rats. Nano emodin treatment decreased the enhanced expression of TNF-R1 in the DRG of T2DM rats and inhibited P2X3 receptor-mediated DNP in T2DM rats. Activation of the ERK pathway is associated with P2X3 receptor-mediated pain signaling [27, 28]. ATP acts via the facilitated P2X3 receptor to cause the phosphorylation of ERK and induce pain [27, 28]. In the present study, the IOD ratio of p-ERK1/2 to ERK1/2 in the DRG of the T2DM group was higher than in the control group. The IOD ratio of p-ERK1/2 to ERK1/2 in T2DM rats treated with nano emodin was significantly lower than in the untreated T2DM group. Therefore, nano emodin treatment relieved P2X3 receptor-mediated hyperalgesia and was related to decreased activation of ERK1/2 in the DRG of T2DM rats.

HEK293 cells are able to express exogenous receptors, and these cells are amenable to many kinds of transfection procedures, permitting the expression of proteins for different purposes [41]. Thus, the HEK293 cell line has been extensively used as an expression tool for recombinant proteins. To investigate whether nano emodin could specifically act on the P2X3 receptor, currents activated by the P2X3 agonist α,β-meATP were recorded with or without nano emodin in HEK293 cells transfected with the pEGFP-hP2X3 plasmid. Our data showed that nano emodin significantly inhibited α,β-meATP-activated currents in HEK293 cells transfected with P2X3 receptor. The electrophysiological results combined with downregulation of P2X3 mRNA and protein after nano emodin treatment confirmed that nano emodin inhibited the transmission of nociceptive signaling by acting on the P2X3 receptor. Therefore, the attenuating effects of nano emodin on mechanical and thermal hyperalgesia in T2DM rats were related to downregulation of P2X3 receptor in the DRG.

Conclusions

Nano emodin treatment decreased upregulation of P2X3 receptor, TNF-α protein, and the phosphorylation of ERK1/2 in the T2DM DRG. Downregulation of P2X3 receptor was associated with decreased thermal and mechanical hyperalgesia in T2DM rats. These results indicate that nano emodin treatment may alleviate the DNP by inhibiting excitatory transmission mediated by the P2X3 receptor in DRG neurons.

Funding information These studies was supported by grants (Nos.: 81570735, 31560276, 81560219, 81171184, 31060139, 81360136, 81360140, 81560529, and 81200853) from the National Natural Science Foundation of China, a grant (Nos.: 20151BBG70250 and 20151BBG70253) from the Technology Pedestal and Society Development Project of Jiangxi Province, a grant (2014-47) from Major Disciplines of Academic and Technical Leaders Project of Jiangxi Province, a grant (No.: 20142BAB205028, 20171BAB205025, and 20142BAB215027) from the Natural Science Foundation of Jiangxi Province, and grants (Nos.: GJJ13155 and GJJ14319) from the Educational Department of Jiangxi Province.

Compliance with ethical standards The procedures were approved by the Animal Care and Use Committee of Nanchang University Medical School.

Conflict of interest The authors declare that they have no conflicts of interest.

References

1. Whiting DR, Guariguata L, Weil C, Shaw J (2011) IDF diabetes atlas: global estimates of the prevalence of diabetes for 2011 and 2030. Diabetes Res Clin Pract 94(3):311–321. https://doi.org/10.1016/j.diabres.2011.10.029
2. Treede RD, Jensen TS, Campbell JN, Cruccu G, Dostrovsky JO, Griffin JW, Hansson P, Hughes R, Nurmikko T, Serra J (2008) Neuropathic pain: redefinition and a grading system for clinical and research purposes. Neurology 70(18):1630–1635. https://doi.org/10.1212/01.wnl.0000282763.29778.59
3. Callaghan BC, Cheng HT, Stables CL, Smith AL, Feldman EL (2012) Diabetic neuropathy: clinical manifestations and current treatments. Lancet Neurol 11(6):521–534. https://doi.org/10.1016/S1474-4422(12)70065-0
4. Schreiber AK, Nones CF, Reis RC, Chichorro JG, Cunha JM (2015) Diabetic neuropathic pain: physiopathology and treatment. World J Diabetes 6(3):432–444. https://doi.org/10.4239/wjd.v6.i3.432
5. Tesfaye S, Boulton AJ, Dyck PJ, Freeman R, Horowitz M, Kempler P, Lauria G, Malik RA, Spallone V, Vinik A, Bernardi L, Valensi P (2010) Diabetic neuropathies: update on definitions, diagnostic criteria, estimation of severity, and treatments. Diabetes Care 33(10):2285–2293. https://doi.org/10.2337/dc10-1303
6. Obrosova IG (2009) Diabetes and the peripheral nerve. Biochim Biophys Acta 1792(10):931–940. https://doi.org/10.1016/j.bbadis.2008.11.005
7. Davies M, Brophy S, Williams R, Taylor A (2006) The prevalence, severity, and impact of painful diabetic peripheral neuropathy in type 2 diabetes. Diabetes Care 29(7):1518–1522. https://doi.org/10.2337/dc05-2228
8. Tavakoli M, Malik RA (2008) Management of painful diabetic neuropathy. Expert Opin Pharmacother 9(17):2969–2978. https://doi.org/10.1517/14656560802498149
9. Morales-Vidal S, Morgan C, McCoyd M, Hornik A (2012) Diabetic peripheral neuropathy and the management of diabetic peripheral neuropathic pain. Postgrad Med 124(4):145–153. https://doi.org/10.3810/pgm.2012.07.2576
10. Singh R, Kishore L, Kaur N (2014) Diabetic peripheral neuropathy: current perspective and future directions. Pharmacol Res 80:21–35. https://doi.org/10.1016/j.phrs.2013.12.005
11. Burnstock G (2007) Physiology and pathophysiology of purinergic neurotransmission. Physiol Rev 87(2):659–797. https://doi.org/10.1152/physrev.00043.2006
12. Gao Y, Xu C, Liang S, Zhang A, Mu S, Wang Y, Wan F (2008) Effect of tetramethylpyrazine on primary afferent transmission mediated by P2X3 receptor in neuropathic pain states. Brain Res Bull 77(1):27–32. https://doi.org/10.1016/j.brainresbull.2008.02.026
13. Gao Y, Liu H, Deng L, Zhu G, Xu C, Li G, Liu S, Xie J, Liu J, Kong F, Wu R, Li G, Liang S (2011) Effect of emodin on neuropathic pain transmission mediated by P2X2/3 receptor of primary sensory neurons. Brain Res Bull 84(6):406–413. https://doi.org/10.1016/j.brainresbull.2011.01.017
14. Liang S, Xu C, Li G, Gao Y (2010) P2X receptors and modulation of pain transmission: focus on effects of drugs and compounds used in traditional Chinese medicine. Neurochem Int 57(7):705–712. https://doi.org/10.1016/j.neuint.2010.09.004
15. Burnstock G (2006) Purinergic P2 receptors as targets for novel analgesics. Pharmacol Ther 110(3):433–454. https://doi.org/10.1016/j.pharmthera.2005.08.013
16. Novakovic SD, Kassotakis LC, Oglesby IB, Smith JA, Eglen RM, Ford AP, Hunter JC (1999) Immunocytochemical localization of P2X3 purinoceptors in sensory neurons in naive rats and following neuropathic injury. Pain 80(1–2):273–282
17. Zhang A, Gao Y, Zhong X, Xu C, Li G, Liu S, Lin J, Li X, Zhang Y, Liu H, Linag S (2010) Effect of sodium ferulate on the hyperalgesia mediated by P2X3 receptor in the neuropathic pain rats. Brain Res 1313:215–221. https://doi.org/10.1016/j.brainres.2009.11.067
18. Lin J, Li G, Den X, Xu C, Liu S, Gao Y, Liu H, Zhang J, Li X, Liang S (2010) VEGF and its receptor-2 involved in neuropathic pain transmission mediated by P2X(2)(/)(3) receptor of primary sensory neurons. Brain Res Bull 83(5):284–291. https://doi.org/10.1016/j.brainresbull.2010.08.002
19. Ueno S, Moriyama T, Honda K, Kamiya H, Sakurada T, Katsuragi T (2003) Involvement of P2X2 and P2X3 receptors in neuropathic pain in a mouse model of chronic constriction injury. Drug Develop Res 59(1):104–111. https://doi.org/10.1002/ddr.10208
20. Xu GY, Li G, Liu N, Huang LY (2011) Mechanisms underlying purinergic P2X3 receptor-mediated mechanical allodynia induced in diabetic rats. Mol Pain 7:60. https://doi.org/10.1186/1744-8069-7-60
21. Hanani M, Blum E, Liu S, Peng L, Liang S (2014) Satellite glial cells in dorsal root ganglia are activated in streptozotocin-treated rodents. J Cell Mol Med 18(12):2367–2371. https://doi.org/10.1111/jcmm.12406
22. Messinger RB, Naik AK, Jagodic MM, Nelson MT, Lee WY, Choe WJ, Orestes P, Latham JR, Todorovic SM, Jevtovic-Todorovic V (2009) In vivo silencing of the Ca(V)3.2 T-type calcium channels in sensory neurons alleviates hyperalgesia in rats with streptozocin-induced diabetic neuropathy. Pain 145(1–2):184–195. https://doi.org/10.1016/j.pain.2009.06.012
23. Gunduz O, Oltulu C, Buldum D, Guven R, Ulugol A (2011) Anti-allodynic and anti-hyperalgesic effects of ceftriaxone in streptozocin-induced diabetic rats. Neurosci Lett 491(1):23–25. https://doi.org/10.1016/j.neulet.2010.12.063
24. Xu C, Xu W, Xu H, Xiong W, Gao Y, Li G, Liu S, Xie J, Tu G, Peng H, Qiu S, Liang S (2012) Role of puerarin in the signalling of neuropathic pain mediated by P2X3 receptor of dorsal root ganglion neurons. Brain Res Bull 87(1):37–43. https://doi.org/10.1016/j.brainresbull.2011.10.007
25. Xu H, Wu B, Jiang F, Xiong S, Zhang B, Li G, Liu S, Gao Y, Xu C, Tu G, Peng H, Liang S, Xiong H (2013) High fatty acids modulate P2X(7) expression and IL-6 release via the p38 MAPK pathway in PC12 cells. Brain Res Bull 94:63–70. https://doi.org/10.1016/j.brainresbull.2013.02.002
26. Liu S, Zou L, Xie J, Xie W, Wen S, Xie Q, Gao Y, Li G, Zhang C, Xu C, Xu H, Wu B, Lv Q, Zhang X, Wang S, Xue Y, Liang S (2016) LncRNA NONRATT021972 siRNA regulates neuropathic pain behaviors in type 2 diabetic rats through the P2X7 receptor in dorsal root ganglia. Mol Brain 9:44. https://doi.org/10.1186/s13041-016-0226-2
27. Burnstock G, Krugel U, Abbracchio MP, Illes P (2011) Purinergic signalling: from normal behaviour to pathological brain function. Prog Neurobiol 95(2):229–274. https://doi.org/10.1016/j.pneurobio.2011.08.006
28. Seino D, Tokunaga A, Tachibana T, Yoshiya S, Dai Y, Obata K, Yamanaka H, Kobayashi K, Noguchi K (2006) The role of ERK signaling and the P2X receptor on mechanical pain evoked by movement of inflamed knee joint. Pain 123(1–2):193–203. https://doi.org/10.1016/j.pain.2006.02.032
29. Barriere DA, Rieusset J, Chanteranne D, Busserolles J, Chauvin MA, Chapuis L, Salles J, Dubray C, Morio B (2012) Paclitaxel therapy potentiates cold hyperalgesia in streptozotocin-induced diabetic rats through enhanced mitochondrial reactive oxygen species production and TRPA1 sensitization. Pain 153(3):553–561. https://doi.org/10.1016/j.pain.2011.11.019
30. Peng H, Zou L, Xie J, Wu H, Wu B, Zhu G, Lv Q, Zhang X, Liu S, Li G, Xu H, Gao Y, Xu C, Zhang C, Wang S, Xue Y, Liang S (2017) lncRNA NONRATT021972 siRNA decreases diabetic neuropathic pain mediated by the P2X3 receptor in dorsal root ganglia. Mol Neurobiol 54(1):511–523. https://doi.org/10.1007/s12035-015-9632-1
31. Wang S, Xu H, Zou L, Xie J, Wu H, Wu B, Yi Z, Lv Q, Zhang X, Ying M, Liu S, Li G, Gao Y, Xu C, Zhang C, Xue Y, Liang S (2016)

LncRNA uc.48+ is involved in diabetic neuropathic pain mediated by the P2X3 receptor in the dorsal root ganglia. Purinergic Signal 12(1):139–148. https://doi.org/10.1007/s11302-015-9488-x

32. Burnstock G (2006) Pathophysiology and therapeutic potential of purinergic signaling. Pharmacol Rev 58(1):58–86. https://doi.org/10.1124/pr.58.1.5
33. Burnstock G (2009) Purinergic receptors and pain. Curr Pharm Des 15(15):1717–1735
34. Burnstock G (2014) Purinergic signalling: from discovery to current developments. Exp Physiol 99(1):16–34. https://doi.org/10.1113/expphysiol.2013.071951
35. Stein C, Clark JD, Oh U, Vasko MR, Wilcox GL, Overland AC, Vanderah TW, Spencer RH (2009) Peripheral mechanisms of pain and analgesia. Brain Res Rev 60(1):90–113. https://doi.org/10.1016/j.brainresrev.2008.12.017
36. Xu JT, Xin WJ, Zang Y, Wu CY, Liu XG (2006) The role of tumor necrosis factor-alpha in the neuropathic pain induced by Lumbar 5 ventral root transection in rat. Pain 123(3):306–321. https://doi.org/10.1016/j.pain.2006.03.011
37. Thomas P, Smart TG (2005) HEK293 cell line: a vehicle for the expression of recombinant proteins. J Pharmacol Toxicol Methods 51(3):187–200. https://doi.org/10.1016/j.vascn.2004.08.014